J. Ind. Geophys. Union, 29(1) (2025), 38-44

Impact of solar activity on ~200-year cyclic variations in groundwater recharge rates in the Badain Jaran Desert, Inner Mongolia, Northwest China

Rajesh Rekapalli[1,2], R.K.Tiwari[1] and Animesh Mandal[3]
[1]CSIR-National Geophysical Research Institute, Hyderabad-500007, India
[2]AcSIR- National Geophysical Research Institute, Hyderabad-500007, India
[3]Indian Institute of Technology, Kanpur-208016, India

ABSTRACT

Understanding groundwater recharge variations is crucial for assessing the impact of climatic and solar influences on water resources. We attempt here to quantify the cyclic solar forcing on groundwater recharge rate (GRR) through the analysis of ~ 700 years of GRR data from the dry lands of the Badain Jaran Desert in Northwest China and Total Solar Irradiance (TSI) data using principal component analysis and statistical methods. Our results confirm a significant role of solar activity in groundwater recharge variations. Singular spectrum analysis of GRR and TSI time series reconstructed from the first three principal modes, revealed common spectral peaks, indicating a significant influence of solar activity on GRR. We observed that a small portion of solar variation (~ 0.021%) of TSI appeared in the second and third eigenmodes of TSI, is found to be responsible for the ~200-year cyclic variability. Approximately 33.66% of the GRR variability is attributed to long-term solar activity trends, while 11.81% is associated with the ~200-year Suess solar cycle. Additionally, residual spectral analysis suggests potential influences of shorter solar cycles (63±10 years, 33±3 years, 24±2 years, and 18±2 years) and non-linear solar phenomena. Thus, this study provides critical insights into the coupling between solar activity and groundwater recharge, emphasizing the importance of long-term and cyclic solar influences, in modeling future groundwater scenarios under changing climatic conditions.

Keywords: Groundwater recharge rate, Spectrum analysis, Total Solar Irradiance, Eigenmode, Badain Jaran Desert.

INTRODUCTION

Understanding changes in groundwater recharge is crucial for society, as it requires analyzing the sensitivity of recharge processes to both internal and external factors that influence groundwater availability. These changes are predominantly driven by climatic variations, with temperature, precipitation, and evapotranspiration being among the key factors. Numerous studies have explored the potential links between climate change and water resources (Goderniaux et al., 2009; Green et al., 2011; Newcomer et al., 2014; Rossman et al., 2014; Zhang et al., 2014; Shamir et al., 2015). A detailed statistical or mathematical analysis to identify trends and cyclic patterns in long-term groundwater fluctuation rates, as well as their potential links to influencing processes, is crucial for improving the modeling of groundwater recharge. Since groundwater recharge is increasingly recognized as a proxy for climate change, such an analysis would provide valuable insights into climate and environmental changes. Researchers have compared groundwater recharge rate (GRR) data with various climatic indicators, including tree rings, unsaturated zone profiles, and sunspot numbers, to explore these relationships (Gates et al., 2008; Tiwari and Rajesh, 2014).

Tiwari and Rajesh (2014) have shown evidence of a ~200-year solar suess cycle and its impact on the long-term groundwater recharge rates by analyzing proxy reconstructed GRR (Gates et al., 2008) and Sunspot Number (Solanki et al, 2004) data. They have suggested that ~48% of the recharge is controlled by this ~200-year solar cycle. However, in the above study, a quantified relationship between solar energy (TSI) and GRR was not established. According to them, during the reversal phase of sunspot, the increased TSI through facular excess emission (Frohlich, 2000, 2009) enhances the evaporation of surface water and thereby reduces the infiltration. Such an increase in TSI will also cause a change in the timing and intensity of precipitation, which might affect the groundwater recharge. However, the TSI data was not used in their study to quantify the percentage of TSI variation that drives the groundwater recharge rate variation at ~200-year periodicity. Therefore, in the present study, we use advanced statistical and spectral methods to identify the significant correlations between GRR and TSI, to estimate the percentage of TSI variation responsible for ~200-year cyclic variation in GRR.

METHODS AND DATA SOURCES

Singular Spectrum Analysis (SSA)

The time series X(t) of length N is embedded into the trajectory matrix $T_{l\times k}$ using an appropriate window length ‘l’ guided by weighted correlation (here k=N-l+1). In the next step, we apply singular value decomposition to decompose the trajectory matrix into eigenvectors and eigenvalues as shown in Equation 1.

$$T = \sum_{i=1}^{d} \sqrt{\lambda_i} U_i V_i^T \qquad (1)$$

Where λ_i is the ith Eigen value corresponding to the ith eigenvector U_i of TT^T. The triple ($\sqrt{\lambda_i}, U_i, V_i$) is called the ith Eigen triple and d is the number of Eigen triples with nonzero Eigenvalues. We identify the significant individual and paired Eigen triplets from proper analysis of Eigen spectrum and Eigenvectors for principal component/Eigenmode reconstruction. From these identified Eigen triplets, we reconstruct the trajectory matrix using the following equation 2.

$$Tr = \sum_{G} \sqrt{\lambda_i}\, U_i V_i^T \quad (2)$$

Here the summation is over the selected Eigen triplets denoted by group G. Finally, the Eigenmodes / principal components can be obtained through the diagonal averaging of the reconstructed trajectory matrix (Vautard and Ghil, 1989; Golyandina et al., 2001; Tiwari and Rajesh, 2014; Rekapalli and Tiwari, 2015).

Eigen weighted cross-correlation

Although the qualitative analysis of eigenmodes of different data sets explains the physical process and relationship between them, cross-correlation coefficients help to quantify the relation. Pearson's cross-correlation coefficients are computed between the principal/eigenmodes of two-time series data to identify their association or dynamical influences. The cross-correlation coefficients between different eigenmodes are generally calculated by giving equal weight to each Eigenmode. However, we have noticed a problem with the standard sample cross-correlation coefficient calculation approach as different eigenmodes contribute differently to the entire process. We suggested a new approach in which Eigenvalues are introduced as weights in the correlation coefficient computation to overcome the above (Rajesh and Tiwari, 2018). Eigen weighted cross-correlation coefficient (ECC) between Eigenmodes A and B of two different time series with eigenvalue percentages 'a' and 'b' is given as

$$c_{net} = \frac{c * (a + b)}{2} \quad (3)$$

Here 'c' is the sample cross-correlation coefficient between the eigenmodes A and B. The following example illustrates the above idea. Consider the cross-correlation coefficient estimated between two modes of respective eigenvalue percentages 0.2 and 0.5 is 0.9. However, this value (i.e., 0.9) may not suggest a strong correlation between the two data sets because the Eigenmodes with 0.2 and 0.5 eigenvalue percentages represent 20% and 50% of the respective time series. Hence, we propose the above formula (eq. 3) for more accurate quantification of Eigenmode correlations that signify the physical relationship between the source data.

If we use equation (1) for the above example, the net Eigen weighted correlation between the two eigenmodes with eigenvalue percentages 0.2 and 0.5 respectively and a standard cross-correlation of 0.9 is

$$c_{net} = \frac{0.9 * (0.2 + 0.5)}{2} = 0.315$$

If a single eigenmode from the first dataset correlates with multiple eigenmodes from the second dataset, the net correlation coefficient is calculated by summing the correlation coefficients of all individual correlating pairs. This net correlation gives us the quantitative estimate for the physical relationship between two processes related to the two Eigenmodes.

Groundwater recharge rate (GRR) data

Groundwater recharge history (mm/year) of 700 years reconstructed using the mass balance of chloride from densely sampled homogeneous profile (Edmunds et al., 2006) of the unsaturated zone, taken from Gates et al (2008), is used in the present analysis (Tiwari and Rajesh, 2014). According to Gates et al (2008), the timing of decadal or century-scale fluctuations cannot be reliably discerned due to the uncertainty in chloride (CL) inputs. Hence, the groundwater recharge record may show some resolution problems and phase errors (Gates et al, 2008; Tiwari and Rajesh, 2014). However, the recharge history shows the wet periods around AD 1380, 1580, and 1750, approximately with ~ 200-year intervals with dominant quasi-periodic dry phases in between. Also, some intermittent short-term wet and dry periods were observed between 1800 – 1900 (Tiwari and Rajesh, 2014).

Total Solar Irradiance (TSI) data

The TSI data used in the present study is part of 9300 years of solar irradiance reconstructed from the open solar magnetic field, estimated from cosmogenic radionuclide ^{10}Be (Steinhilber et al., 2008, 2009) measured in ice cores GRIP (Vonmoos et al., 2006) and South Pole (McCracken et al., 2004), besides neutron monitor count rates (Usoskin et al., 2005). The data at 5 years resolution are re-sampled from 40-year running means. This is one of the best available TSI data to test the claimed links between groundwater recharge rate and TSI.

RESULTS and DISCUSSION

Role of solar activity on groundwater recharge

The raw data of GRR and TSI (Figures 1a and 1b) show a common long-term trend along with superimposed short-term nonstationary oscillations. Pearson's correlation coefficient of 0.61 was noticed between the groundwater recharge rate and TSI raw data sets. SSA allows us to scrutinize such complex data to identify independent principal modes for physical interpretation. The GRR and TSI data (Fig. 1) are decomposed using the SSA method using the window length of 40 and 200 years respectively. We have estimated these window length values using the weighted correlation method (Tiwari and Rajesh, 2014; Tiwari et al., 2016). The statistical validation of errors and resolution of the GRR and TSI data are systematically verified and discussed by us and by several other researchers (Gates et al, 2008; Steinhilber et al., 2008, 2009; Tiwari and Rajesh, 2014). The first three principal modes of GRR and TSI data sets represent the long periodic trend and oscillatory components. Hence, we analyze the GRR and TSI signals reconstructed from the first three principal modes shown in Figure 2a (Tiwari and Rajesh, 2014) to demonstrate the relationship between GRR and TSI. The amplitude of ~200-year periodic variation in GRR increased gradually from 1305 to 1985. But, the amplitude of the ~ 200-year cyclic mode of TSI gradually decreased from 1305 to 1985. One can visually see from Figure 2a that the peak changes appeared in GRR amplitudes (maximum to minimum) during the lowest TSI variation. The standard sample cross-correlation (Box et al., 1994) along with the p-value of the Null hypothesis rejection test for randomness in correlation and Eigen-weighted cross-correlation coefficients computed between the SSA reconstructed signals (Fig. 2a) at different Lags are shown in Figure 2b. The sample cross-correlation coefficient is higher compared to Eigen-weighted cross-correlation coefficients. The cyclic pattern observed in the correlation analysis (Fig. 2b) attests to the common ~200-220-year periodic component in both data sets as discussed in our previous study (Tiwari and Rajesh, 2014). The shift in peak cross-correlation from zero value may be either due to errors in the dating process or the 40-year running average used in the reconstruction of TSI data. However, as we are not interested in searching for the periodic oscillations of periods less than 40 years, the lag observed in the cross-correlation is not significant enough to influence our results. Further, Figure 2c and Figure 2d show the spectrum of SSA-reconstructed GRR and TSI signals respectively. The spectrum of GRR and TSI data reveal dominant common spectral peaks at periods of ~200±20 (Suess cycle), and 512±25 (Trend) years with more than 99% confidence levels (Tiwari et al., 2016). Hence, our results suggest a persuasive role of solar activity on groundwater recharge rate via a long-term trend and ~200±20-year solar Suess cycle.

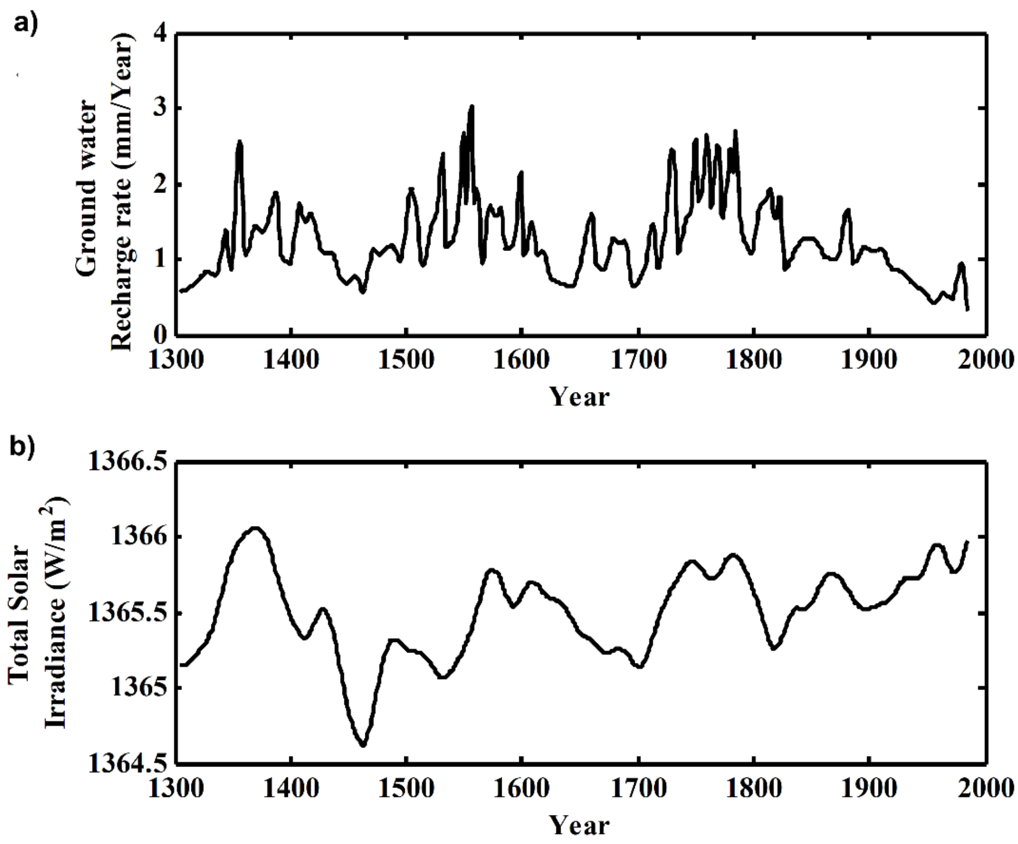

Figure 1. Raw data of (**a**) Groundwater recharge rates, and (**b**) Total Solar Irradiance data

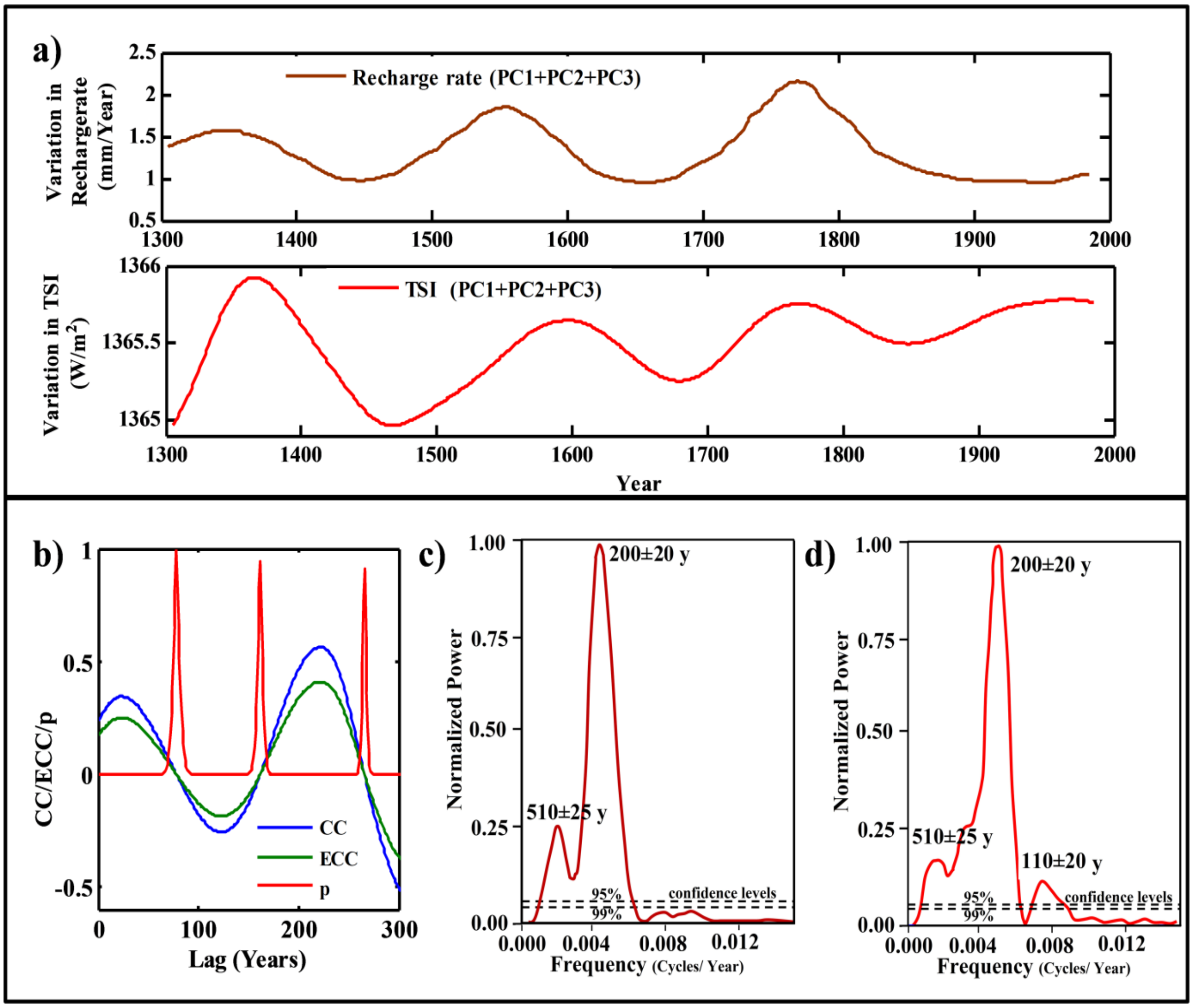

Figure 2. (**a**) Groundwater recharge rate (top panel) and total solar irradiance (bottom panel) data reconstructed using SSA from principal components 1 to 3. (**b**) Correlation coefficients estimated using conventional cross-correlation (CC) along with the probability (p) estimated for the rejection of null hypothesis and Eigen weighted cross-correlation (ECC). (**c**) Spectrum of SSA reconstructed recharge rate data. (**d**) Spectrum of SSA reconstructed TSI data

Sensitivity of 200-year groundwater cycle to TSI variation

As discussed above, TSI influences the GRR via long-term trend and ~200±20 year Suess cycle. The first Eigenmodes of GRR and TSI data shown in Figure 3a, contribute nearly 33.66% and 99.94% variance of total recharge and solar irradiance respectively and also depict long-term trends. The trend components of GRR and TSI seem to be part of long periodic cycles with periodicity greater than or equal to the length of the data, which is not discernible here (Rekapalli and Tiwari, 2020). The first mode of GRR correlates well with the long-term trend of TSI with an eigen-weighted correlation coefficient of 0.52 (sample cross-correlation coefficient: 0.79) as shown in Figure 3b. Eigen weighted cross-correlation coefficient suggests that the forcing by the trend of the TSI on GRR is quite significant for modeling future patterns of groundwater recharge scenarios. Unlike groundwater recharge, solar irradiance follows cycles up to million-year periodicities or greater (Tiwari, 2005). The trend in the TSI replicates the parts of several long periodic solar cycles. Hence, it is inappropriate to conclude that the 99.94% variability in the first principal component of TSI is responsible for the observed 33.66% variability in the GRR. In the future, the availability of longer records may allow for discerning the percentage of solar irradiance responsible for 33.66% variability in the GRR. However, we infer here that the 33.66% groundwater recharge rates do not follow the ~200-year solar cycle and may be regarded as a part of some higher-order cycles.

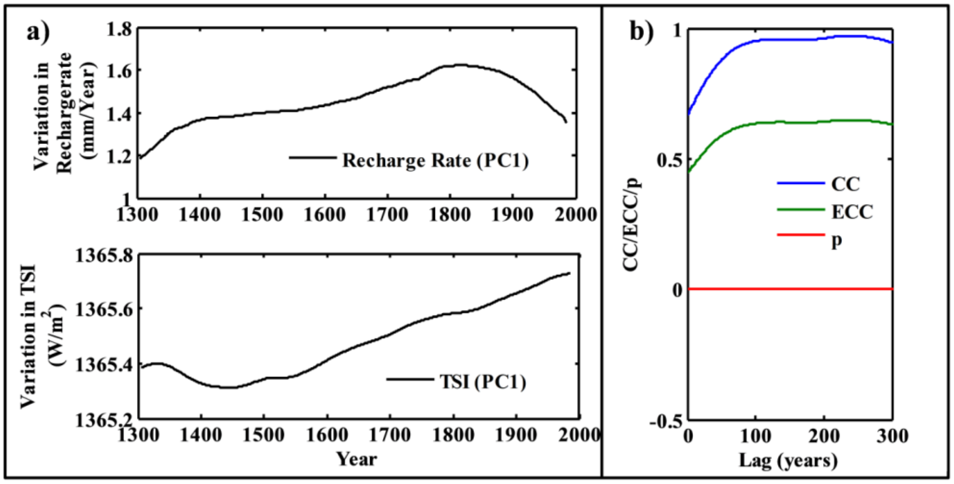

Figure 3. (**a**) The first principal component of Groundwater recharge rate (PC1) and TSI (PC1) reconstructed using SSA. (**b**) Cross-correlation coefficient (CC) along with the probability (p) for rejection of null-hypothesis on their correlation (red line) and Eigen weighted cross-correlation coefficient (ECC) computed between first principal components of GRR and TSI.

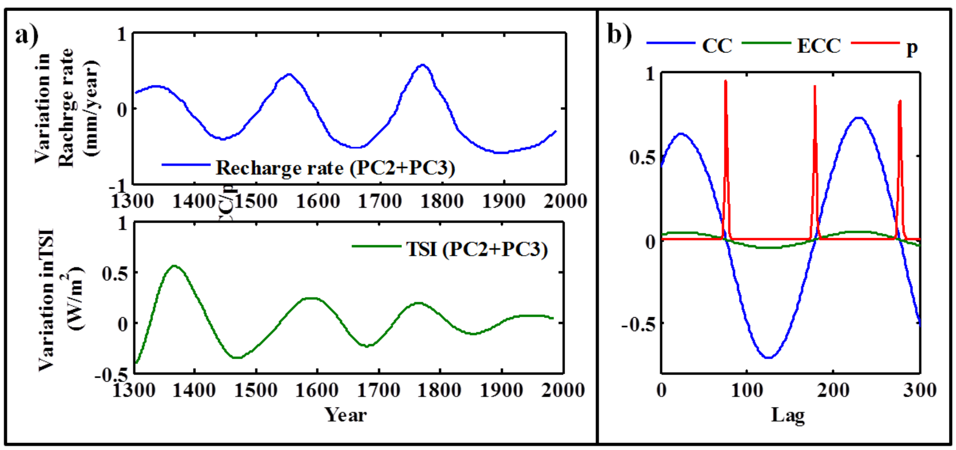

Figure 4. (**a**) Variation in Groundwater recharge rate (PC2+PC3) and TSI (PC2+PC3) reconstructed using SSA. (**b**) Cross-correlation coefficient (CC) along with the probability of Null hypothesis rejection (red line) and Eigen weighted cross-correlation coefficient (ECC) of Groundwater recharge rate (PC2+PC3) and TSI(PC2+PC3).

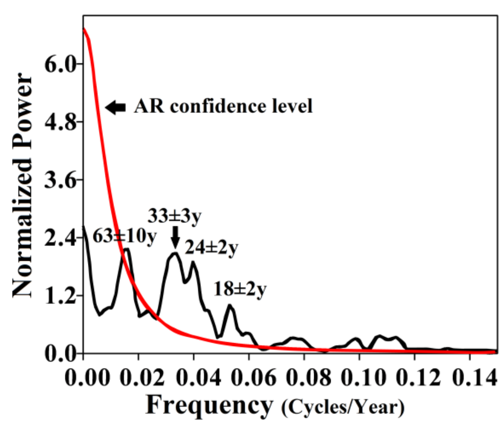

Figure 5. The power spectrum of the residual GRR signal was reconstructed from eigen modes 2 to 40 using SSA, which depicted the spectral peaks at some solar and other nonlinear periods due to beats and modulations.

The second and third modes of TSI (0.012%, 0.009%) and GRR (6.45%, 5.36%) shown in Figure 4a, are cyclic with a periodicity of ~200-205 years. There is a gradual increase in the amplitude of this cycle in GRR from 1305 to 1985 whereas, a gradual decrease in the ~200-year cyclic component of TSI. This suggests the enhanced groundwater recharge conditions due to the reduction in the evapotranspiration of surface water, caused by reduced surface temperatures during low TSI. The cross-correlation along with the null hypothesis probabilities and Eigen Weighted cross-correlation estimated at different lags, are shown in Figure 4b. The pure cyclic nature of the correlation suggests the existence of the same periodicity in both data sets. The peak correlation is observed at lag 23. From the eigenvalue percentage of these modes, only 0.021% of total solar irradiance is responsible for such a ~200 cyclic variation (11.81%) in the groundwater recharge. A sample correlation coefficient of 0.63 was noticed between the SSA reconstructed signal (from PC2 and PC3) of GRR and TSI. However, low-value eigen-weighted cross-correlation suggests (0.044) relatively low significance of this mode (only 11.81% of the total variance) in the groundwater recharge. This year solar cycle is prominent in many paleoclimate indicators (Tiwari, 2005). The correlation of climate processes with solar activity has been pervasive in the past 10,000 years, especially in dry and wet spells (Verschuren et al., 2000; Zang et al., 2008; Lean, 2010). Several studies inferred the ~200-year solar cycle as a dominant and important cycle that influenced the Earth’s climate during Holocene (Eddy, 1976; Vasilev et al., 1999; Muscheler et al., 2003; Tiwari, 2005).

Although Tiwari and Rajesh (2014) have successfully discussed the first three eigenmodes in the GRR data, the contribution of 54.53% residual signal to the total GRR was not analyzed. Finally, we estimated the spectral content of the residual (PC4 to PC40) of GRR as shown in Figure 5. We have computed an Auto Regression (AR) based confidence level to avoid the influence of erratic noise present in the record. The spectral peaks identified with 63±10y, 33±3y, and 24±2y, are consistent and may correspond to some lower-order solar periods. The component with 18±2y may be due to some nonlinear phenomenon of solar components as discussed in Scafetta (2012). The spectral analysis of residual signals, within the limits of the data resolution, also stands as evidence of solar forcing on groundwater recharge rates. Chapanov et al. (2017) calculated the decadal harmonics of TSI, LOD-Length Of Day, MSL-Mean Sea Level precipitation, and temperature over Eastern Europe are analyzed using models of the Jose, de Vries, and Suess cycles (periods: 178.7, 208, and 231 years) and their phase differences. The periodic decadal cycles (e.g., 33.0, 29.7, 25.7, 23.1 years) seen in the modeling results highlight solar-terrestrial interactions. This further suggests the role of solar-terrestrial interactions on the decadal cycles observed in GRR residual.

CONCLUSIONS

We analyzed the principal components/eigenmodes in the 700-year record of groundwater recharge rate data from China along with solar activity (Total Solar Irradiance) using a new eigen-weighted cross-correlation method to report the percentage of solar radiation that is responsible for observed trends and cyclic patterns in GRR. Our result suggests that only 11.81% of GRR is associated with the solar Suess cycle. A part of GRR (33.66%) is associated with the long-term trend in solar activity. A small fraction i.e., 0.021% of the total solar radiation is responsible for the observed 200±10y cyclic groundwater recharge variations. Although the data resolution is limited, the residual analysis revealed the influence of short-term solar periods and some non-linear beating phenomena on groundwater recharge rates from China.

Acknowledgments

We thank the Director, CSIR-NGRI for his kind permission to publish this work. We acknowledge Prof. John. B. Gates for groundwater recharge rate data and Prof. F. Steinhilber for TSI data. (Ref: NGRI/Lib/2024/Pub-138)

Author Credit Statement

Rajesh Rekapalli: Conceptualization, methodology, formal analysis, interpretation and writing the original draft and edits. R. K. Tiwari: Interpretation and writing the original draft and edits. Animesh Mandal: Interpretation and writing the original draft and edits.

Data Availability

The data sets used in this study are can be accessed from the sources cited in the manuscript.

Compliance with Ethical Standards

The authors declare no conflict of interest and adhere to copyright norms.

REFERENCES

Box, G. E. P., Jenkins, G. M. and Reinsel, G. C., 1994. Time Series Analysis: Forecasting and Control. 3rd ed. Englewood Cliffs, NJ: Prentice Hall.

Chapanov, Y., Ron, C. and Vondrak, J., 2017. Decadal cycles of Earth rotation, mean sea level and climate, excited by solar activity. Acta Geodyn. Geomater, 14, 241-250.

Eddy, J. A., 1976. The Maunder Minimum: The reign of Louis XIV appears to have been a time of real anomaly in the behavior of the sun. Science, 192(4245), 1189-1202.

Edmunds, W. M., Ma, J., Aeschbach-Hertig, W., Kipfer, R. and Darbyshire, D. P. F., 2006. Groundwater recharge history and hydrogeochemical evolution in the Minqin Basin, North West China. Appl. geochemistry, 21(12), 2148-2170.

Frohlich, C., 2000. Observations of Irradiance Variations. Space Sci. Rev., 94(1-2), 15-24.

Fröhlich, C., 2009. Observational evidence of a long-term trend in total solar irradiance. Astron. Astrophys., 501, 27–30, doi:10.1051/0004-6361/200912318.

Gates, J. B., Edmunds, W. M., Ma, J. and Sheppard, P. R., 2008. A 700-year history of groundwater recharge in the drylands of NW China. The Holocene, 18(7), 1045-1054.

Goderniaux, P., Brouyere, S., Fowler, H.J., Blenkinsop, S., Therrien, R., Orban, P. and Dassargues, A., 2009. Large scale surface-subsurface hydrological model to assess climate change impacts on groundwater reserves. J. Hydrology, 373, 122–138. doi:10.1016/j. jhydrol.2009.04.017

Golyandina, N., Nekrutkin, V. and Zhigljavsky, A. A., 2001. Analysis of time series structure: SSA and related techniques. CRC press

Green, T.R., Taniguchi, M., Kooi, H., Gurdak, J.J., Allen, D.M., Hiscock, K.M., Treidel, H. and Aureli, A., 2011. Beneath the surface of global change: impacts of climate change on groundwater. J. Hydrology, 405, 532–560.

Lean, J. L., 2010. Cycles and trends in solar irradiance and climate. Wiley interdisciplinary reviews: climate change, 1(1), 111-122.

McCracken, K.G., McDonald, F.B., Beer, J., Raisbeck, G. and Yiou. F., 2004. A phenomenological study of the long term cosmic ray modulation, 850-1958AD. J. Geophys. Res., 109, A12103, doi:10.1029/2004JA010685

Muscheler, R., Beer, J. and Kromer, B., 2003. Long-term climate variations and solar effects. Proceedings of the ISCS 2003 on Solar Variability as an Input to the Earth's Environment, vol. 535, pp. 305-316

.Newcomer M.E., Gurdak, J.J., Sklar, L.S. and Nanus, L., 2014. Urban recharge beneath low impact development and effects of climate variability and change. Water Resour. Res., 50, 1716–1734

Rajesh, R. and Tiwari, R.K., 2018. Impact of solar cycles on groundwater recharge on decadal to centennial scale: A case study from Northwest China. Abstract volume, 55th Annual Convention of Indian Geophysical Union, Dec 2018, p14.

Rekapalli, R. and Tiwari, R. K., 2015. A short note on the application of Singular Spectrum Analysis for Geophysical Data processing. J. Ind. Geophys. Union 19(1), 77-85.

Rekappali, R. and Tiwari R.K., 2020. Breaks in linear trends or parts of cycles?, Pure Appl. Geophys. 177 (2020), 5469–5474, https://doi.org/10.1007/s00024-020-02577-y

Rossman, N.R., Zlotnik, V.A., Rowe, C.M. and Szilagyi, J., 2014. Vadose zone lag time and potential 21st century climate change effects on spatially distributed groundwater recharge in the semi-arid Nebraska Sand Hills. J. Hydrology 519, 656-669.

Scafetta, N., 2012. Multi-scale harmonic model for solar and climate cyclical variation throughout the Holocene based on Jupiter–Saturn tidal frequencies plus the 11-year solar dynamo cycle. J. Atmosph. Solar-Terrestrial Phys., 80, 296-311.

Shamir, E., Megdal, S.B., Carrillo, C., Castro, C.L., Chang, H.I., Chief, K., Corkhill, F.E., Eden, S., Georgakakos, K.P., Nelson, K.M. and Prietto, J., 2015. Climate change and water resources management in the Upper Santa Cruz River, Arizona. J. Hydrology, 521, 18-33.

Solanki, S. K., Usoskin, I. G., Kromer, B., Schüssler, M. and Beer, J., 2004. Unusual activity of the Sun during recent decades compared to the previous 11,000 years. Nature, 431(7012), 1084-1087.

Steinhilber, F., Abreu, J. A. and Beer, J.,2008. Solar modulation during the Holocene. Astrophys. Space Sci. Trans., 4, 1-6

Steinhilber, F., Beer, J. and Fröhlich, C., 2009. Total solar irradiance during the Holocene. Geophys. Res. Lett., 36, L19704, doi:10.1029/2009GL040142.

Tiwari, R. K., 2005. Geo-spectroscopy. Capital Publishing Company.

Tiwari, R. K. and Rajesh, R., 2014. Imprint of long-term solar signal in groundwater recharge fluctuation rates from Northwest China. Geophys. Res. Lett., 41(9), 3103-3109.

Tiwari, R. K., Rajesh, R. and Padmavathi, B., 2016. Evidence of Higher-Order Solar Periodicities in China Temperature Record. Pure Appl. Geophys., 1-10.

Usoskin, I.G., Alanko-Huotari, K., Kovaltsov, G.A. and K. Mursula. 2005. Heliospheric modulation of cosmic rays: Monthly reconstruction for 1951-2004. J. Geophys. Res., 110, A12108, doi:10.1029/2005JA011250

Vasil'ev, S. S., Dergachev, V. A. and Raspopov, O. M., 1999. Sources of long-term variations in the radiocarbon concentration in the earth's atmosphere. Geomag. Aeronomy, 39(6), 749.

Vautard, R. and Ghil, M., 1989. Singular spectrum analysis in nonlinear dynamics, with applications to paleoclimatic time series. Physica, D 35, 395-424.

Verschuren, D., Laird, K.R. and Cumming, B.F., 2000. Rainfall and drought in equatorial east Africa during the past 1100 years. Nature, 403, 410–414.

Vonmoos, M., Beer, J. and Muscheler, R., 2006. Large variations in Holocene solar activity: Constraints from 10Be in the Greenland Ice Core Project ice core. J. Geophys. Res., 111, A10105, doi:10.1029/2005JA011500

Zhang, P., Cheng, H., Edwards, R. L., Chen, F., Wang, Y., Yang, X.et al., 2008. A test of climate, sun, and culture relationships from an 1810-year Chinese cave record. Science, 322(5903), 940-942.

Zhang, Y., Wang, J.C., Jing, J.H. and Sun, J.C., 2014. Response of groundwater to climate change under extreme climate conditions in North China Plain. J. Earth Sci. China, 25, 612–618.

Received on: 11-06-2024 ; Revised on: 08-01-2025 ; Accepted on: 08-01-2025